IEEE Photonics Journal
An IEEE Photonics Society Publication

Compact Optical Generation of Microwave Signals Using a Monolithic Quantum Dot Passively Mode-Locked Laser

Volume 1, Number 4, October 2009

C.-Y. Lin, Student Member, IEEE
Y.-C. Xin, Member, IEEE
J. H. Kim, Student Member, IEEE
C. G. Christodoulou, Fellow, IEEE
L. F. Lester, Senior Member, IEEE

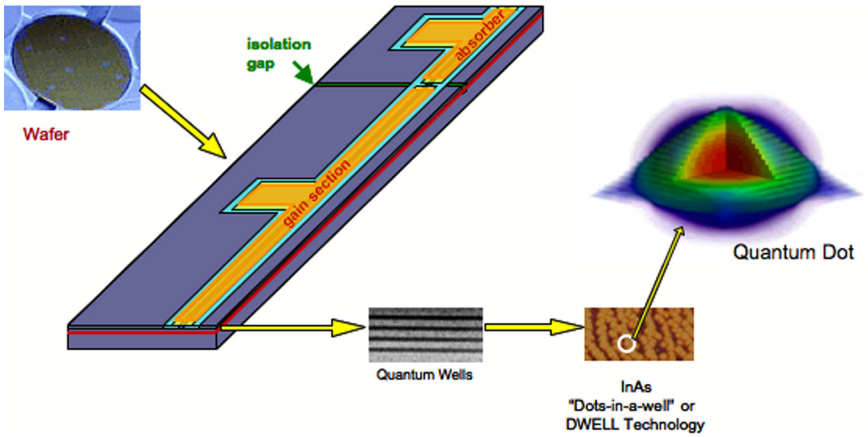

DOI: 10.1109/JPHOT.2009.2035523
1943-0655/$26.00 ©2009 IEEE

Compact Optical Generation of Microwave Signals Using a Monolithic Quantum Dot Passively Mode-Locked Laser

C.-Y. Lin,[1] *Student Member, IEEE*, Y.-C. Xin,[2] *Member, IEEE*, J. H. Kim,[3] *Student Member, IEEE*, C. G. Christodoulou,[3] *Fellow, IEEE*, and L. F. Lester,[1] *Senior Member, IEEE*

[1]Center for High Technology Materials, University of New Mexico, Albuquerque, NM 87106, USA
[2]IBM Systems &Technology Group, Semiconductor Solutions, Hopewell Junction, NY 12533, USA
[3]Department of Electrical and Computer Engineering, University of New Mexico, Albuquerque, NM 87106, USA

DOI: 10.1109/JPHOT.2009.2035523
1943-0655/$26.00 ©2009 IEEE

Manuscript received September 28, 2009; revised October 20, 2009. First published Online October 30, 2009. Current version published November 17, 2009. This work supported by the Air Force Office of Scientific Research under Grants FA9550-06-1-0411 and FA9550-09-1-0490. Corresponding author: C. Y. Lin (e-mail: cylin@unm.edu).

Abstract: Microwave signal generation from the saturable absorber of a monolithic quantum dot passively mode-locked laser is presented. We observe a differential efficiency of 33% that measures the optical-to-RF power conversion. An optimum extraction efficiency of the saturable absorber of about 86% is also found. To assess the stability of the device, the mode-locking operation regime of the quantum dot device is analyzed and compared to the quantum well system. Our findings confirm that quantum dot mode-locked lasers are suitable candidates for the optical generation of RF signals in a compact and efficient semiconductor device.

Index Terms: Mode-locked lasers, multifrequency antennas, reconfigurable architectures, semiconductor lasers.

1. Introduction

Due to the global interest in higher frequency bandwidths, producing compact RF signal sources on a chip is a key research topic for applications such as the wireless communication field, software-defined radio, radar, and satellite communication systems. Monolithic passively mode-locked lasers (MLLs) are promising candidates for microwave generation [1]–[3] because of their compact size, low power consumption, direct electrical pumping, and high electrical-to-optical-to-electrical (E/O/E) conversion efficiency. Several unique advantages of quantum dot (QD) materials, such as their ultrabroad bandwidth, feedback resistance, ultrafast gain dynamics, and easily saturated gain and absorption, make them an ideal choice for monolithic semiconductor MLLs [4]–[7]. These characteristics give QDMLLs the advantage of pulse stability over a wider power range than their quantum well (QW) counterparts. Previous semiconductor active regions such as QWs could produce the same optical gain and absorption functions, but frequently required separate optimization of the optical materials in the MLL cavity. The QDMLL can easily use the *same* epitaxial layer structure in both the absorber and gain sections [8]–[10].

Conventionally, optical generation of microwave signals can be achieved by using two different laser sources applied to a photodetector or a photomixer made from low-temperature-grown GaAs [11]. The beat signal with a required frequency equivalent to the spacing of the two wavelengths is

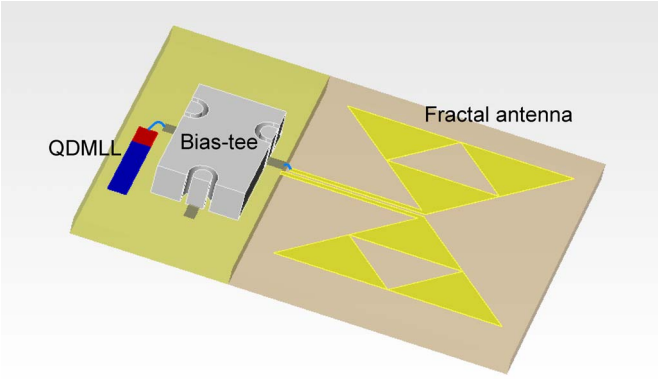

Fig. 1. Integration of the QDMLL with a reconfigurable bowtie antenna. First, high-frequency electrical pulse signals are generated from the saturable absorber of the QDMLL. These signals are next routed by a bias tee and a coplanar waveguide to a reconfigurable bowtie antenna. This integrated unit can then be used as a cellular block in more complex arrays that are controlled, for example, by field-programmable gate arrays.

extracted from the output of the photodetector. This approach is called optical heterodyning or photomixing. The advantage of this technique is the wide tunability of the output frequency from near DC to the terahertz range. However, the drawback is the relatively low conversion efficiency and frequency stability issue. Several groups have contributed toward improving the conversion efficiency and maintaining high stability in heterodyned systems [12]–[16]. In this previous research, optical injection locking or an optical phase-locked loop was implemented to reduce the phase noise and maintain high stability [12], [13]. However, in this case, a high-quality microwave reference signal is also required. Thus, it is hard to apply this technique to a wireless communication system in which no reference signal is available for the local oscillator. To avoid using a reference signal, the beat signal at the output of a photodetector is generated by a single laser source that has either a single wavelength with dual longitudinal modes [14], [15] or two wavelengths operating in single longitudinal mode for each wavelength [16].

In this work, we combine the optical pulse generation of a passive MLL with the high-speed characteristics of the QD saturable absorber (SA) to produce a microwave signal directly from the same laser diode. From the RF point of view, the SA behaves as a p-i-n photodetector. When an optical pulse train passes through the SA, an electrical pulse is directly generated at the same repetition rate as the optical pulses using *only DC bias*. This compact RF signal generator can then be integrated with a reconfigurable antenna that accesses the various frequencies available from the pulsed source. Fig. 1 shows an example of this hybrid integration, which has been described elsewhere [2].

Here, we focus on the characterization and conversion efficiency of the RF signal generation through the SA of a passive QDMLL. The antenna design and integration strategy will be discussed in another publication. This paper is organized as follows. Section 2 is devoted to the laser structure and the RF generation mechanism. The experimental setup and RF signal characterization are presented in Section 3. In Section 4, the derivation of equations related to the conversion efficiency of the QDMLL's optical output into electrical pulse is described. The experimental and calculated results are discussed in Section 5, and the key findings and future work are summarized in Section 6.

2. Device Structure and RF Generation Mechanism

The laser epitaxial structure of this device is a multistack "Dots-in-a-WELL" (DWELL) structure that is composed of an optimized six-layer QD active region grown by solid-source molecular beam epitaxy on a (001) GaAs substrate [17]. The p- and n-type AlGaAs cladding layers have 20% Al content, and graded interfaces are used between the clads and the GaAs waveguide layer

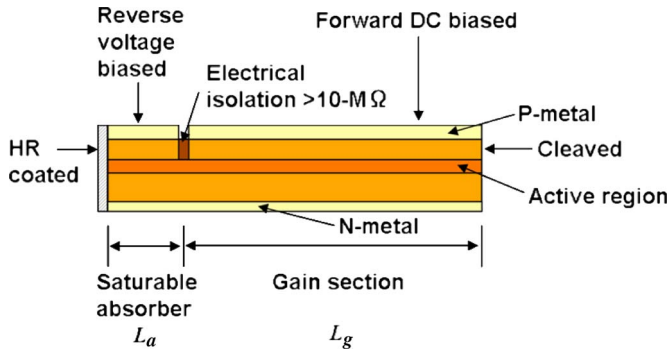

Fig. 2. Schematic diagram of the two-section passive MLL (side view).

surrounding the DWELL structure. The 3.5-μm-wide optical ridge-waveguide devices are fabricated following standard dry-etch, planarization, and metallization processing. In this work, the two-section QD passive MLLs are made with a total cavity length of 4.1 mm and a SA length of 0.8 mm. A highly reflective (HR) coating $(R_1 \approx 95\%)$ is applied to the mirror facet next to the SA and the other facet is cleaved $(R_2 \approx 32\%)$. Fig. 2 shows a schematic diagram of a two-section passive MLL.

Typically, the electrical pulse train can be generated using a low-temperature (LT) metal-semiconductor-metal (MSM) detector that converts the optically generated pulse from MLL to an RF output signal [18]. However, an alternative approach that we favor for optically generating the RF frequencies is to bypass the LT-MSM detector entirely and use the transient photocurrent produced in the SA of the passive QDMLL as the microwave signal source [2]. This device layout is simpler and has the potential to convert the ultrafast optical signal to electrical pulses more efficiently. As a picosecond optical pulse goes into the SA, the leading edge of the optical pulse is absorbed and creates free carriers. The resulting electrons and holes are swept to the metal contacts as the photocurrent due to the built-in electrical field. This process has the potential to be very fast since absorbers composed of QDs have demonstrated subpicosecond recovery times [4], [8]. Most likely the speed of the electrical impulse from the absorber section will be limited by electrical parasitics that can be reduced by decreasing the bonding pad capacitance or the length of the absorber itself. Normally, decreasing the length of the absorber would diminish the optical-to-electrical conversion efficiency as in any waveguide-based photodetector. However, in the passive MLL geometry, the ability to apply HR coatings to both mirror facets is a significant advantage for realizing simultaneous high speed and high efficiency. In our first example presented here, only one laser mirror is HR coated for simplicity.

3. QDMLL Device Characterization

This section describes the basic output characteristics of the QDMLL and the operating parameters of the devices that are necessary for evaluating the DC to RF differential efficiency as shown in Section 4. Fig. 3 shows the total loss data as a function of the emission wavelength using an improved segmented contact method [19]. From Fig. 3, the internal loss of the optical waveguide is found to be 2 cm^{-1}. Fig. 4 is the light-current (LI) curve of the laser for various absorber biases of the 4.1-mm device. The maximum slope efficiency is 0.27 W/A with 0 V applied to the absorber. The inset of Fig. 4 demonstrates the single-section laser diode case for comparison. To realize this layout, the anodes of the gain and absorber section were tied together through wire bonding and then pumped uniformly. The differential quantum efficiency of the laser diode can be determined through this layout. The optical spectrum under 200-mA DC bias on the gain section and 0 V applied to the absorber is shown in Fig. 5. The peak lasing wavelength is at 1.21 μm and the mode-locked 3-dB spectral bandwidth is about 2.8 nm with a typical pulse width on the order of 10 ps and an RMS timing jitter of 1–2 ps calculated from the offset range of 30 kHz to 30 MHz [20]. Under the condition of complete mode locking, which was confirmed by optical pulse measurement from a

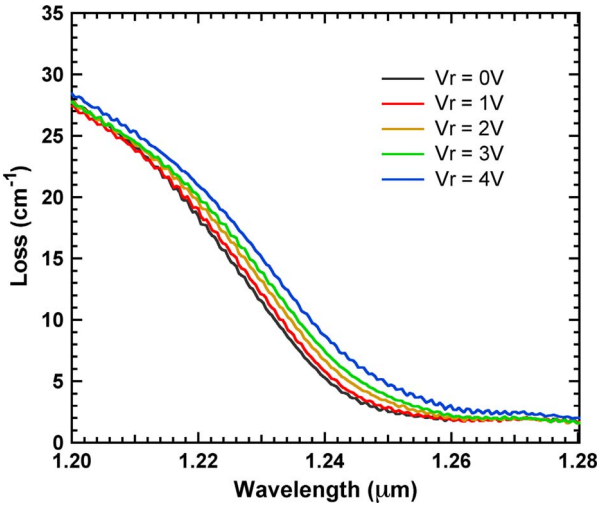

Fig. 3. Room-temperature total loss spectra of the QDMLL device as measured by the multisection technique.

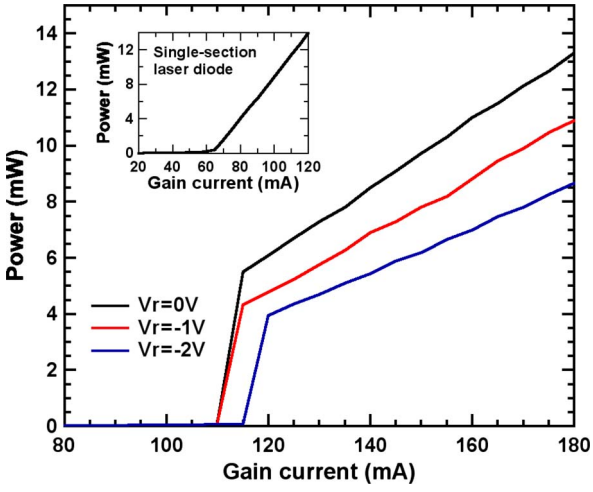

Fig. 4. LI curve of the laser for various absorber biases from 0 V to −2 V. The inset shows a single-section uniformly pumped case.

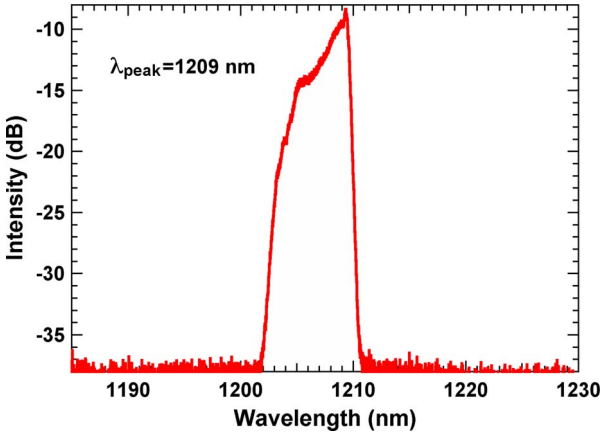

Fig. 5. Optical spectrum of the QDMLL device under 2000-mA DC bias on the gain section and 0 V applied to the absorber.

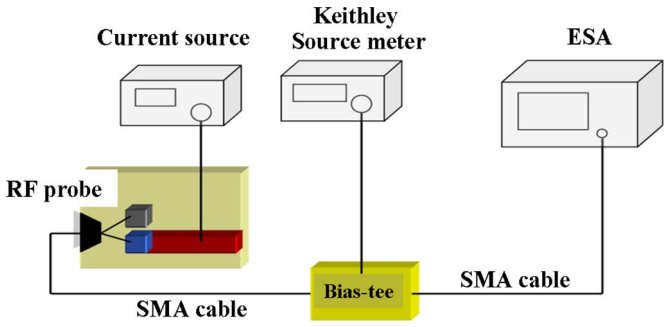

Fig. 6. Apparatus of the RF signal measurement.

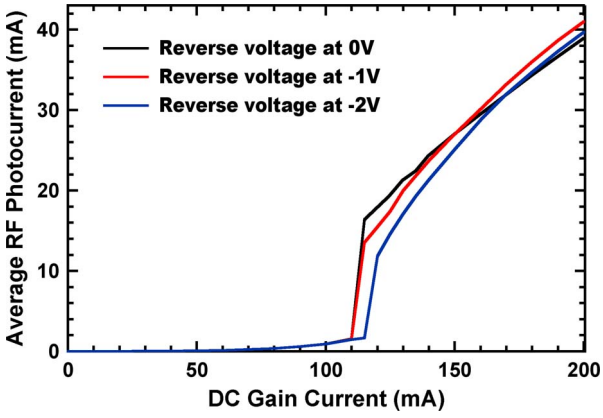

Fig. 7. Average RF photocurrent generated in the saturable absorber of the QDMLL as a function of the DC current applied to the gain section of the laser for various absorber biases.

background-free Femtochrome autocorrelator, the measured current from the SA is the average RF photocurrent. The RF power spectrum was measured using the setup shown in Fig. 6 using high-speed RF probing. The series connection of a bias tee and an on-wafer RF probe was used to apply the reverse voltage on the SA and to extract the microwave signal from the QDMLL simultaneously. Fig. 7 shows that the average RF photocurrent is on the order of 40 mA when up to 200 mA of DC current is injected into the gain section. The maximum DC current for this study is limited to 200 mA to avoid deleterious heating of the device. Fig. 8 also demonstrates an RF power of -2 dBm under 200-mA DC bias on the gain section and -1 V applied to the absorber. Thus, these RF current pulses can generate a reasonable amount of power that can be transmitted by a reconfigurable bowtie antenna for microwave applications [2], [3]. In general, more power can be directed to the fundamental harmonic by increasing the current bias of the device above 200 mA because this situation expands the pulse width of the QDMLL which favors the baseline frequency.

Another primary advantage of the QDMLL is the expanded range of stable mode locking [17] that permits wider bias operation over which to extract RF signals from the device. The stable bias condition for mode locking was investigated, and the operating regime was mapped out using the gain current and SA reverse voltage as control parameters as seen in Fig. 9. Compared to the QWMLL used for RF generation, the monolithic passive QDMLL clearly demonstrates a mode-locking operation over a wider range of gain currents and absorber voltages [21].

4. Derivation of the Conversion Efficiency of the Passive QDMLL

The design strategy for microwave signal generation from the QDMLL is different from the approach for short optical pulse generation. Since optical power output is not desirable for maximizing the RF

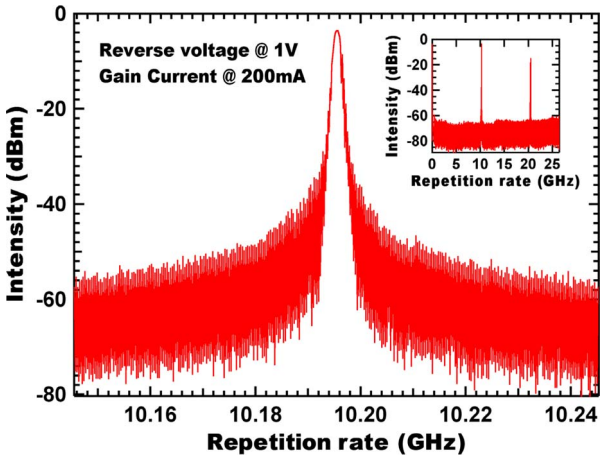

Fig. 8. RF power spectrum of the electric pulse signal directly extracted from the saturable absorber. The resolution bandwidth: 1 MHz.

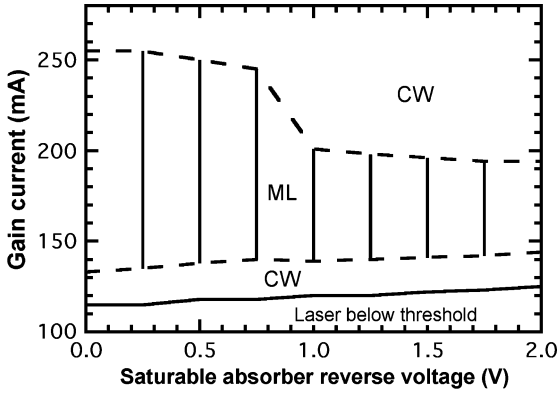

Fig. 9. Operating regime map for 4.1-mm passive QDMLL device. CW: continuous wave.

output from the absorber, different coating concerns and bias conditions are necessary to maximize the electrical pulse output while maintaining the mode-locking operation. As derived below, lowering the mirror loss, α_m, by implementing HR coatings improves the conversion of DC power to RF output power. Another change is that the reverse bias and the length of the absorber should be increased as much as possible at the expense of optical output power since these approaches directly benefit the RF power generation.

The DC-to-RF differential efficiency, η_{DCRF}, or "conversion efficiency" is found by measuring the change in the average RF photocurrent as a function of the DC gain current above threshold. η_{DCRF} is about 33% as calculated from Fig. 7 under the optimum bias condition of -2 V applied to the absorber. This value compares favorably with that demonstrated by the optical heterodyning approach that is commonly used to produce microwave signals. The typical power conversion efficiency of the optical heterodyning is around 2% at the millimeter-wave region [11].

Another important parameter related to the conversion efficiency is the extraction efficiency, η_E, of the SA. Since the epitaxial layer structure is normally designed for the efficient operation of the laser, which seeks to maximize the *injection* efficiency, the extraction efficiency of the reverse-biased absorber is not necessarily optimized. Unlike the conversion efficiency, the extraction efficiency is not directly measurable in the MLL. In order to derive an expression for η_E so that it can be calculated from other measurements, the differential quantum efficiency, η_d, which can be determined from a uniformly pumped laser diode, is found first. (This uniformly

pumped case is experimentally realized by tying the anodes of the SA and gain sections together.) η_d, is defined as

$$\eta_d = \frac{q}{h\nu} \times \frac{\Delta P}{\Delta I} \tag{1}$$

where q is the electronic charge, h is the Planck's constant, ν is the optical frequency, and $\Delta P/\Delta I$ is the slope above the threshold from the LI curve as found in the inset of Fig. 4. The injection efficiency of the laser diode, η_i, is then calculated using η_d and the loss from the waveguide and mirror facets according to the following relation:

$$\eta_i = \eta_d \cdot \frac{\alpha_i + \alpha_m}{\alpha_m} \tag{2}$$

where α_i is the internal loss of the waveguide which can be derived from the loss measurement, α_m is the mirror loss of the laser device, $\alpha_m = (1/2L)\ln(1/R_1R_2)$, and L is the total cavity length. For our QD diode laser material, η_i is 0.63 calculated from all the parameters given above.

After all the basic device parameters are calculated from the single-section case, the various two-section bias conditions that produce mode locking need to be analyzed. The convention here is to quote the bias current on the gain section and the reverse voltage on the absorber section of the MLL. For the two-section laser, the differential quantum efficiency is measured at a fixed reverse voltage on the absorber. For instance, the differential quantum efficiency of the QDMLL under -1-V reverse voltage bias to the SA, η_{d_1V} is denoted as

$$\eta_{d\_MLL} = \eta_{d\_1V} = \frac{q}{h\nu} \times \frac{\Delta P_{1V}}{\Delta I_{1V}}. \tag{3}$$

Next, the expression for the injection efficiency, (2), has to be modified to take into account the optical loss induced by the SA of the MLL

$$\eta_i = \eta_{d\_1V} \times \frac{\alpha_i + \alpha_m + \alpha_{ave\_abs} \times \frac{L_a}{L}}{\alpha_m} \tag{4}$$

where L_a is the length of the SA and α_{ave_abs} is the time-averaged loss of the SA. Since the injection efficiency is the same for the uniformly pumped laser and the MLL, rearranging (4) allows the calculation of the time-averaged loss according to the following expression:

$$\alpha_{ave\_abs} = \frac{L}{L_a}\left[\alpha_m\left(\frac{\eta_i}{\eta_{d\_MLL}} - 1\right) - \alpha_i\right]. \tag{5}$$

Next, from the definition of the DC-to-RF differential efficiency above, we can express η_{DCRF} mathematically as the following equation:

$$\eta_{DCRF} = \eta_i \times \eta_E \times \frac{\alpha_{ave\_abs} \times \frac{L_a}{L}}{(\alpha_i + \alpha_m) + \alpha_{ave\_abs} \times \frac{L_a}{L}}. \tag{6}$$

The ratio on the right-hand side of (6) represents the fraction of the optical power that is converted into electron-hole pairs (EHPs) in the absorber. η_E is then the fraction of EHPs in the absorber that are collected at the external electrodes of the device as photocurrent. Finally, after rearranging (6), the extraction efficiency of the SA can be described by the following relation:

$$\eta_E = \frac{\eta_{DCRF}}{\eta_i \alpha_{ave,abs}}\left(\frac{\alpha_i L}{L_a} + \frac{\alpha_m L}{L_a} + \alpha_{ave,abs}\right). \tag{7}$$

5. Results and Discussion on the Conversion Efficiency

The device parameters and the conversion efficiency analysis results are summarized in Table 1 for different reverse voltages applied to the SA. For reverse voltages greater than 2 V, the mode

TABLE 1
Device parameters and the conversion efficiency result

Reverse voltage on SA	0V	1V	2V
η_d (%)	13	11	9.3
α_{ave_abs} (1/cm)	20	25	33
η_{DCRF} (%)	25	32	33
η_E (%)	75	86	79

locking starts to degrade due to excessive absorption. According to the experimental data and equations derived above, the average η_E of the SA is about 80% as calculated from (7). The extraction efficiency is not noticeably voltage dependent indicating that the carriers are nearly or at velocity saturation in the SA for all biases. The time-averaged loss of the SA rises from 20 to 33 cm^{-1}, depending upon the reverse voltage of the SA, which is consistent with the Stark shift of the absorption edge as a function of increasing electric field across the QDs. The time-averaged loss values are also generally consistent with the measured 1209-nm absorption data shown in Fig. 3. The values at 1209 nm are chosen for comparison because this is the peak lasing of the QDMLL as presented in Fig. 5. The time-averaged loss result for the 2-V reverse voltage case is somewhat larger than that reported in Fig. 3, which is probably due to device heating that decreases the energy gap as the absorber collects a larger current density for increasing reverse bias. It is noted that the overall trend in the conversion efficiency, η_{DCRF}, mirrors that of the time-averaged loss with reverse bias on the SA. This result is to be expected since the ratio on the right-hand side of (6) maximizes at about 65% for a reverse voltage of 2 V. In other words, 65% of the optical power is going into the absorber at this bias. Increasing the number of QD stacks in the active region could potentially increase the power collected by the SA. However, this approach requires increasing the active region thickness, which would cause more EHP recombination that would lower the extraction efficiency. Increasing the width of the active layer could also undesirably broaden the pulse width of the QDMLL because of a longer carrier transit time across the absorber.

It is noted that the extraction efficiency actually exceeds the injection efficiency of 63%, which is probably due to the choice of 20% Al content in the AlGaAs cladding layers and the graded interfaces. The heterojunction offsets between the core and clad layers are probably not large enough for good carrier confinement and optimal injection efficiency in the laser, but this smaller energy offset is obviously beneficial to the transport of carriers in the absorber. In the future, alternative passive QDMLL layouts will be investigated with different QD stack numbers and cladding composition to optimize the conversion efficiency.

6. Conclusion

Compared to the conventional optical heterodyning method, the larger conversion efficiency and easier frequency stabilization of the generated RF frequency from a monolithic passive QDMLL is presented. The optical generation of microwave signals from the passive QDMLL decreases the uncorrelated phase noise and temperature fluctuations that are undesirable effects for wireless communication applications. 33% DC-to-RF conversion efficiency and 86% extraction efficiency of the SA are reported. The tradeoffs in optimizing the laser injection efficiency, absorber extraction efficiency, and the power collected by the absorber were discussed. The extraction-injection efficiency product could be improved through choices of different alloy composition in the cladding layer and QD stacks in the active region. Various laser structures will be tested in the near future. The QDMLL device clearly demonstrates a wider ML operating region compared to the QWMLL used for the RF signal source. On the other hand, phase noise is also a critical issue for wireless application. The QD laser diode has less phase noise compared to QW system because of less spontaneous emission noise in the cavity [20]. Further experimental investigation is required to

analyze the timing jitter of the RF signal through the phase noise measurement. With all the advantages shown above, the monolithic passive QDMLL will be a promising candidate of the compact RF signal source in wireless communication applications.

References

[1] A. J. C. Vieira, P. R. Herczfeld, A. Rosen, M. Ermold, E. E. Funk, W. D. Jemison, and K. J. Williams, "A mode-locked microchip laser optical transmitter for fiber radio," *IEEE Trans. Microw. Theory Tech.*, vol. 49, no. 10, pp. 1882–1887, Oct. 2001.

[2] J. H. Kim, C. G. Christodoulou, Z. Ku, Y.-C. Xin, N. A. Naderi, and L. F. Lester, "Quantum-dot laser coupled bowtie antenna," in *Proc. IEEE AP-S*, Jul. 2008, pp. 1–4.

[3] D. J. Derickson, R. J. Helkey, A. Mar, J. G. Wasserbauer, and J. E. Bowers, "Microwave and millimetre-wave signal generation using modelocked semiconductor lasers with intrawaveguide saturable absorbers," in *Proc. IEEE Int. Symp. Microw. Theory Tech.*, 1992, vol. 2, pp. 753–756.

[4] E. U. Rafailov, M. A. Cataluna, and W. Sibbett, "Mode-locked quantum-dot lasers," *Nat. Photon.*, vol. 1, no. 7, pp. 395–401, Jul. 2007.

[5] M. G. Thompson, A. R. Rae, M. Xia, R. V. Penty, and I. H. White, "InGaAs quantum-dot mode-locked laser diodes," *IEEE J. Sel. Topics Quantum Electron.*, vol. 15, no. 3, pp. 661–672, May/Jun. 2009.

[6] F. Grillot, C.-Y. Lin, N. A. Naderi, M. Pochet, and L. F. Lester, "Optical feedback instabilities in a monolithic InAs/GaAs quantum dot passively mode-locked laser," *Appl. Phys. Lett.*, vol. 94, no. 15, p. 153 503, Apr. 2009.

[7] H. Su, A. L. Gray, R. Wang, T. C. Newell, K. J. Malloy, and L. F. Lester, "High external feedback resistance of laterally loss-coupled distributed feedback quantum dot semiconductor lasers," *IEEE Photon. Technol. Lett.*, vol. 15, no. 11, pp. 1504–1506, Nov. 2003.

[8] D. B. Malins, A. Gomez-Iglesias, S. J. White, W. Sibbett, A. Miller, and E. U. Rafailov, "Ultrafast electroabsorption dynamics in an InAs quantum dot saturable absorber at 1.3μm," *Appl. Phys. Lett.*, vol. 89, no. 17, p. 171 111, Oct. 2006.

[9] X. D. Huang, A. Stintz, H. Li, A. Rice, G. T. Liu, L. F. Lester, J. Cheng, and K. J. Malloy, "Bistable operation of a two-section 1.3-μm InAs quantum dot laser—Absorption saturation and the quantum confined Stark effect," *IEEE J. Quantum Electron.*, vol. 37, no. 3, pp. 414–417, Mar. 2001.

[10] X. D. Huang, A. Stintz, H. Li, L. F. Lester, J. Cheng, and K. J. Malloy, "Passive mode-locking in 1.3μm two-section InAs quantum dot lasers," *Appl. Phys. Lett.*, vol. 78, no. 19, p. 2825, May 2001.

[11] E. R. Brown, F. W. Smith, and K. A. McIntosh, "Coherent millimeter-wave generation by heterodyne conversion in low-temperature-grown GaAs photoconductors," *J. Appl. Phys.*, vol. 73, no. 3, pp. 1480–1484, Feb. 1993.

[12] J. Genest, M. Chamberland, P. Tremblay, and M. Tetu, "Microwave signals generated by optical heterodyne between injection-locked semiconductor lasers," *IEEE J. Quantum Electron.*, vol. 33, no. 6, pp. 989–998, Jun. 1997.

[13] Z. F. Fan and M. Dagenais, "Optical generation of a megahertz-linewidth microwave signal using semiconductor lasers and a discriminator-aided phase-locked loop," *IEEE Trans. Microw. Theory Tech.*, vol. 45, no. 8, pp. 1296–1300, Aug. 1997.

[14] M. Hyodo, M. Tani, S. Matsuura, N. Onodera, and K. Sakai, "Generation of millimeter-wave radiation using a dual-longitudinal-mode microchip laser," *Electron. Lett.*, vol. 32, no. 17, pp. 1589–1591, Aug. 1996.

[15] M. Tani, O. Morikawa, S. Matsuura, and M. Hangyo, "Generation of terahertz radiation by photomixing with dual- and multiple-mode lasers," *Semicond. Sci. Technol.*, vol. 20, no. 7, pp. 151–163, Jul. 2005.

[16] X. F. Chen, Z. Deng, and J. P. Yao, "Photonic generation of microwave signal using a dual-wavelength single-longitudinal-mode fiber ring laser," *IEEE Trans. Microw. Theory Tech.*, vol. 54, no. 2, pp. 804–809, Feb. 2006.

[17] Y.-C. Xin, Y. Li, V. Kovanis, A. L. Gray, L. Zhang, and L. F. Lester, "Reconfigurable quantum dot monolithic multi-section passive mode-locked lasers," *Opt. Express*, vol. 15, no. 12, pp. 7623–7633, Jun. 2007.

[18] L. F. Lester, K. C. Hwang, P. Ho, J. Mazurowski, J. Ballingall, J. Sutliff, S. Gupta, J. Whitaker, and S. R. Williamson, "Ultra-fast long-wavelength photodetectors fabricated on low-temperature InGaAs on GaAs," *IEEE Photon. Technol. Lett.*, vol. 5, no. 5, pp. 511–514, May 1993.

[19] Y.-C. Xin, Y. Li, A. Martinez, T. J. Rotter, H. Su, L. Zhang, A. L. Gray, S. Luong, K. Sun, Z. Zou, J. Zilko, P. M. Varangis, and L. F. Lester, "Optical gain and absorption of quantum dots measured using an alternative segmented contact method," *IEEE J. Quantum Electron.*, vol. 42, no. 7, pp. 725–732, Jul. 2006.

[20] L. Zhang, L.-S. Cheng, A. L. Gray, H. Huang, S. Kutty, H. Li, J. Nagyvary, F. Nabulsi, L. Olona, E. Pease, Q. Sun, C. Wiggins, J. C. Zilko, Z. Zou, and P. M. Varangis, "High-power low-jitter quantum-dot passively mode-locked lasers," *Proc. SPIE*, vol. 6115, p. 611 502, Feb. 2006.

[21] M. Passerini, M. Sorel, and P. J. R. Laybourn, "Optimisation and regime characterisation of monolithic semiconductor mode-locked lasers and colliding-pulse mode-locked lasers at microwave and millimeter-wave frequency," *Proc. Inst. Elect. Eng.—Optoelectron.*, vol. 151, no. 6, pp. 508–512, Dec. 2004.